THE JOURNAL OF COMPARATIVE NEUROLOGY 385:230–244 (1997)

Ultrastructural Analysis of Primary Endings in Deaf White Cats: Morphologic Alterations in Endbulbs of Held

D.K. RYUGO,[1,2]* T. PONGSTAPORN,[1] D.M. HUCHTON,[1] AND J.K. NIPARKO[1]
[1]Department of Otolaryngology-Head and Neck Surgery, Center for Hearing Sciences, Johns Hopkins University School of Medicine, Baltimore, Maryland 21205
[2]Department of Neuroscience, Center for Hearing Sciences, Johns Hopkins University School of Medicine, Baltimore, Maryland 21205

ABSTRACT

Changes in structure and function of the auditory system can be produced by experimentally manipulating the sensory environment, and especially dramatic effects result from deprivation procedures. An alternative deprivation strategy utilizes naturally occurring lesions. The congenitally deaf white cat represents an animal model of sensory deprivation because it mimics a form of human deafness called the Scheibe deformity and permits studies of how central neurons react to early-onset cochlear degeneration. We studied the synaptic characteristics of the endbulb of Held, a prominent auditory nerve terminal in the cochlear nucleus. Endbulbs arise from the ascending branch of the auditory nerve fiber and contact the cell body of spherical bushy cells. After 6 months, endbulbs of deaf white cats exhibit alterations in structure that are clearly distinguishable from those of normal hearing cats, including a diminution in terminal branching, a reduction in synaptic vesicle density, structural abnormalities in mitochondria, thickening of the pre- and postsynaptic densities, and enlargement of synapse size. The hypertrophied membrane densities are suggestive of a compensatory response to diminished transmitter release. These data reveal that early-onset, long-term deafness produces unambiguous alterations in synaptic structure and may be relevant to rehabilitation strategies that promote aural/oral communication. J. Comp. Neurol. 385:230–244, 1997.

Indexing terms: auditory nerve; cochlear nucleus; congenital deafness; hearing; synapses

The mechanisms that regulate neuronal change in response to varying levels of activity are largely unknown, although it has been shown that substantial alterations at the cellular level occur following experimental manipulations of afferent activity. In the auditory system, deafening in neonates (Moore and Kowalchuk, 1988; Lustig et al., 1994; Lesperance et al., 1995) or adults (Powell and Erulkar, 1962; Parks, 1979; Trune, 1982; Moore, 1990; Born et al., 1991) produces atrophic changes in the central pathways. The expression of these changes can appear as the rapid atrophy of dendrites (Benes et al., 1977; Deitch and Rubel, 1984; Deitch and Rubel, 1989a,b), somatic shrinkage (Powell and Erulkar, 1962; Parks, 1979; Trune 1982), and altered axonal projections along the central pathway (Nordeen et al., 1983; Moore and Kowalchuk, 1988; Parks et al., 1990). Such changes are much more striking when deafness is induced in neonates compared with in adults (Hashisaki and Rubel, 1989). Acute pharmacologic blockade of electrical activity in the auditory nerve is also capable of producing central structural changes (Sie and Rubel, 1992; Pasic et al., 1994). In contrast to the effects of deprivation, stimulation paradigms, such as conditioning to certain frequencies, produce expanded representations of neural regions that are specific to the conditioning frequencies (e.g., Robertson and Irvine, 1989; Bakin and Weinberger, 1990; Recanzone et al., 1993). These studies emphasize the extent to which the brain is selectively responsive to the type and amount of afferent activity.

Most experimental studies of acoustic deprivation or structural deafferentation have been performed on phenotypically normal subjects. Cochlear ablation, auditory

Grant sponsor: National Institute of Deafness and Other Communication Disorders, National Institutes of Health; Grant number: 5 RO1 DC00232.

*Correspondence to: David K. Ryugo, Center for Hearing Sciences, Johns Hopkins University School of Medicine, 720 Rutland Avenue, Baltimore, MD 21205. E-mail: dryugo@bme.jhu.edu

Received 14 November 1995; Revised 25 February 1997; Accepted 31 March 1997

nerve section, and pharmacologic blockade of the cochlea are known to produce central changes that are hypothesized to result from the deprivation (Rubel and Parks, 1988). These deprivation effects, however, can be complicated by variables, such as indirect insults to the central neural structures by a surgically compromised blood supply or "downstream" neurotoxic actions of drug application. Thus, the conditions of experimentally induced deafness are different from those associated with naturally occurring deafness. In this context, the congenitally deaf animal offers an alternative model of auditory deafferentation and may provide insights into a broader spectrum of variables that affect brain structure and function, particularly as related to early development.

The deaf white cat (DWC) is an animal model that mimics the Scheibe deformity in humans (Bosher and Hallpike, 1965; Deol, 1970; Suga and Hattler, 1970; Brighton et al., 1991). The Scheibe deformity features early-onset, progressive cochleosaccular degeneration and severe sensorineural hearing impairment (Scheibe, 1892). In cats, the defect is transmitted in an autosomal dominant pattern with incomplete penetrance and is identified by pigmentation abnormalities (white coat, heterochromic irides) and cochleosaccular degeneration (Rawitz, 1896; Wolff, 1942; Bosher and Hallpike, 1965; Bergsma and Brown, 1971). The cochleosaccular pathology ranges from hair cell loss to complete collapse of the organ of Corti with variable spiral ganglion cell loss (Bosher and Hallpike, 1965; Mair, 1973; Pujol et al., 1977; Ribillard et al., 1981). Furthermore, there are atrophic structural changes in neurons of the central auditory pathway, which include the cochlear nucleus (West and Harrison, 1973; Larsen and Kirchhoff, 1992; Saada et al., 1996) and superior olivary complex (Schwartz and Higa, 1982).

The cochlear nucleus occupies a key position of the auditory system because it receives incoming signals from cochlear receptors and gives rise to the ascending auditory pathways (Ramón y Cajal, 1909; Lorente de Nó, 1981; Ryugo, 1992). Furthermore, the synaptic interface between endbulbs of Held, the large axosomatic endings of the myelinated auditory nerve fibers, and spherical bushy cells in the cochlear nucleus provides an optimal site for study because the structural components are well defined. Any pathologic changes at this initial stage of signal processing could corrupt the transmission of encoded information prior to its presentation to higher nuclei within the auditory system. Atrophic changes have been well documented for the spherical bushy cells of DWCs (West and Harrison, 1973; Larsen and Kirchhoff, 1992; Saada et al., 1996), and our interest addresses the role played by the presynaptic endings. In the present study, we describe ultrastructural changes in the congenitally DWC that occur at this first-order auditory synapse. By examining the pre- and postsynaptic features of endings, we quantitatively compared the structure of synapses in normal adult and in DWCs by using light and electron microscopy.

MATERIALS AND METHODS

Subjects

Four cats with white coats and a family history of deafness were tested on the day of experimentation by using auditory brainstem evoked responses (ABR); three were bilaterally deaf and one was unilaterally deaf (Table 1). An ear is defined as deaf when no evoked responses to clicks or tones were evident at intensity levels up to 100-dB sound pressure level (SPL). All cats under 8 months of age were from our own colony and were initially tested at 1 month of age. The degree of deafness did not change from this initial test to their final test. The 6.5-year-old DWC was purchased from a colony at Bowman-Gray School of Medicine. We were informed that this cat had early-onset deafness, which was verified by ABR testing at 3 months of age (J. Ryu, personal communication). All cats were free of mange and respiratory problems, exhibited normal motor movements, clear eyes, and intact tympanic membranes, and had clean external and middle ears with no signs of infection upon otoscopic examination. Data from normal cats of previously published studies (Sento and Ryugo, 1989; Ryugo et al., 1996) were reanalyzed and used as comparison data for the deaf cats. All procedures were used in accordance with the guidelines and approval of the Animal Care and the Committee of the Johns Hopkins Medical School.

TABLE 1. Deaf White Cat Subject Data[1]

Cat	Age	Sex	Weight	Hearing (ABR)	No. of EM EBs
DWC 7	6 months	Female	2.5 kg	Bilateral deafness	5
DWC 11	6 months	Male	2.8 kg	Bilateral deafness	2
DWC 8	8 months	Female	3.4 kg	Unilateral deafness	2
DWC 6	6.5 years	Male	4.5 kg	Bilateral deafness	5

[1]ABR, auditory brainstem evoked response; EM, electron microscope; EBs, end bulbs.

Auditory brainstem responses

Each cat had its hearing tested prior to the auditory nerve injection. Behaviorally, the cats did not respond to auditory stimuli (loud handclap from behind). Cats were sedated with 0.9 ml intramuscular ketamine hydrochloride and 0.1 ml intramuscular acepromazine, placed in a soundproof chamber, and sterile needle electrodes were inserted, one behind each ear, one at the vertex, and the ground wire into the nasal dorsum skin. With the use of a standard auditory brainstem evoked response (ABR) protocol with hardware and software (Nicolet/Spirit Evoked Potentials System, Version 1.31), recordings were made between the vertex electrode and the ipsilateral ear. With this particular system, a 20 dB correction factor is needed to convert dB to dB SPL (re: 0.0002 dynos/cm^2). DWCs revealed an absence of waves to clicks and tones (up to 100 dB SPL), indicating that they had significant hearing loss (Fig. 1). In contrast, ABR waveforms from hearing ears were entirely consistent with normal ABR data (Melcher et al., 1996).

Animal preparation

Each cat was initially anesthetized with intramuscular injections of ketamine hydrochloride (0.75 cc) and xylazine hydrochloride (0.25 cc). Atropine (0.25 cc IM) was administered to reduce secretions. Thereafter, supplemental anesthesia with intraperitoneal injections (0.4 cc per kg body weight) of diallyl barbituric acid (100 mg/ml) in urethane solution (400 mg/ml) was administered to maintain areflexia. Body temperature was monitored by rectal thermometer and maintained at approximately 39°C by using a heating pad and heated soundproof chamber.

For each cat, the trachea was cannulated, an intravenous line was placed in the cephalic vein for administration of fluids, and the head placed in a stereotaxic device. The skin and soft tissue were incised over the skull, and

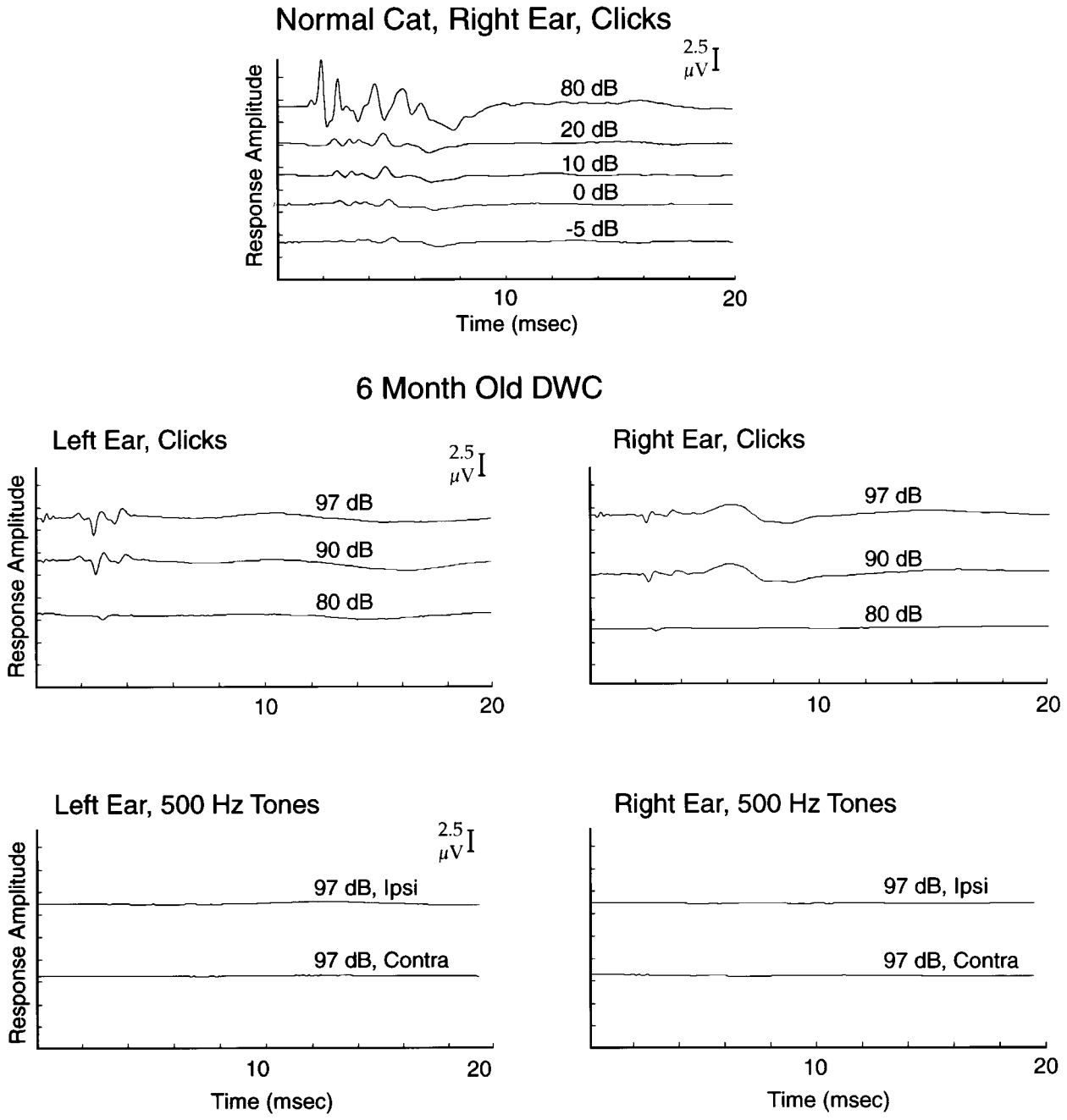

Fig. 1. Auditory brainstem evoked responses (ABRs) from a normal pigmented cat (**top**) and a 6-month-old deaf white cat with blue eyes (**bottom**). The hearing cat exhibits a normal ABR waveform, with thresholds at approximately −5 dB (15 dB SPL). Similar waveforms were recorded from its left ear. In the white cat, ABRs were flat for both click and tone burst stimuli (500 Hz), with thresholds above 80 dB (100 dB SPL) in both ears. Ipsi, ipsilateral; Contra, contralateral.

dissection was continued to each external meatus. The posterior cranial fossa was opened with rongeurs, the cerebellum was exposed, and the dura reflected. The cerebellum was retracted medially to expose the auditory nerve in its course from internal auditory meatus to cochlear nucleus. Glass micropipettes (I.D. 50 μm), filled with a 30% solution of horseradish peroxidase (HRP) in 0.05 Tris buffer (pH 7.6), were inserted into each auditory nerve under direct microscopic control. HRP was injected by passing 5 μA of positive current (50% duty cycle) for 5 minutes through the micropipette into the auditory nerve.

Tissue preparation

Approximately 24 hours after HRP was injected, each cat was given a lethal dose of anesthesia, the heart was exposed, heparin sulfate (0.1 ml) was injected intracardially, and a large bore needle was inserted into the left ventricle for transcardial perfusion. Approximately 250 ml

of 0.1 M phosphate-buffered saline (pH 7.4), containing 0.1% sodium nitrite for dilating the vessels, was perfused into the animal, followed immediately by 1.5 liters of fixative containing 2% paraformaldehyde and 2% glutaraldehyde in 0.1 M phosphate buffer.

Cochleae were perfused through both oval and round windows by using the primary fixative solution, left overnight at 5°C, and dissected out of the skull the following morning. Each cochlea was decalcified for 2 weeks in a solution of 0.1 M ethylenediaminetetraacetic acid (EDTA) with 1% glutaraldehyde, embedded in a gelatin-albumin block, and sectioned on a Vibratome. Midmodiolar sections at a thickness of 50 µm were collected in serial order, mounted on "subbed" slides, air dried overnight, stained with 0.5% cresyl violet, dehydrated in ascending concentrations of ethanol, cleared in xylenes, and coverslipped with Permount.

Each brain was postfixed overnight in fresh fixative, and the next day the brainstems with cochlear nuclei were dissected and embedded in a gelatin-albumin mixture hardened with glutaraldehyde. Modified parasagittal sections (oriented parallel to the lateral surface of the nuclei) were cut at a thickness of 50 µm on a Vibratome. Sections were collected in 0.1 M phosphate buffer, kept in serial order, and washed in the same buffer several times, and kept refrigerated at 4°C overnight. The next morning, sections were incubated for 60 minutes in phosphate buffered 0.05% 3,3′-diaminobenzidine (DAB, Sigma, St. Louis, MO, grade II Tetra HCl) activated with 0.01% hydrogen peroxide. Sections were then washed several times with 0.1 M phosphate buffer.

The tissue for electron microscopy was placed in 1% OsO_4 for 15 minutes, rinsed multiple times in 0.1 M maleate buffer (pH 5.0), and stained in 1% uranyl acetate (4°C) overnight. The following morning, the sections were again washed with 0.1 M maleate buffer, dehydrated in increasing concentrations of ethanol, soaked in propylene oxide, infiltrated with Epon, and embedded in fresh Epon between sheets of Aclar (Ted Pella, Inc., Redding, CA). Hardened sections were taped to labeled microscope slides for examination with a light microscope. Selected areas in the anteroventral cochlear nucleus (AVCN) were drawn with the aid of a light microscope and drawing tube at both high and low magnifications, with particular attention paid to HRP-labeled endbulbs and surrounding landmarks.

Relevant labeled structures were identified and dissected from individual sections and reembedded in BEEM capsules for electron microscopic analysis. Serial ultrathin sections of approximately 75 nm thickness were collected on Formvar-coated grids, stained with 7% uranyl acetate, and viewed and photographed with a JEOL 100CX electron microscope. Total magnification for ultrastructural analysis was ×70,000. Because each ultrathin section represents a thin slice through each endbulb, only parts of the endbulb can appear in any section. These parts are referred to as ending profiles, and multiple series of consecutive sections (10–35) were analyzed for two or three endbulbs per cat.

Data collection and analysis

Every HRP-labeled endbulb from DWC-6 (n = 20) and DWC-7 (n = 32) was drawn and analyzed for light microscopy. Four labeled endbulbs and one unlabeled endbulb were randomly selected from each of the above cats and used for electron microscopic analysis. For unknown reasons, we did not recover HRP-labeled auditory nerve fibers in the other cats (DWC-8 and DWC-11). Nevertheless, endbulbs are so distinctive at the ultrastructural level that they can be identified even without intracellular label, so two unlabeled endbulbs from each of these other DWCs were randomly selected for quantitative EM study. All endbulbs analyzed in this report were located in the anterior division of the AVCN (Cant and Morest, 1979), where they made synaptic contact with a spherical bushy cell.

The HRP-labeled endbulbs were drawn with the aid of a light microscope and drawing tube at a total magnification of ×2,500 (×100 oil immersion lens, NA = 1.25). The silhouette of reconstructed endbulbs was digitized, the area calculated, and the fractal index computed by using the box counting technique (Smith et al., 1989; Porter et al., 1991). Silhouette area was used to represent endbulb size. Fractal geometry has been successfully applied as a quantitative descriptor of the complexity of natural structures and growth processes (Mandelbrot, 1982), and we used it to assess endbulb complexity (Fractal Dimension Calculator, Version 1.5). The method applied in the present report used a grid of square boxes having various side sizes (s, in pixels) placed over the outline of the endbulb. The number of boxes N(s) that contained part of the endbulb was counted. The fractal dimension D is given by the slope of the linear portion of the graph where log (N(s)) is plotted against log (1/s), derived from the relationship: log (N(s)) = D log(1/s). Because there is no preferred origin for the boxes with respect to the pixels in the image, multiple measures N(s) were computed from different box origins, and the graphed value of N(s) is the average of N(s) from nine different origins. Fractal values range between 1 and 2, and because the fractal index is represented on a logarithmic scale, each increase of 0.1 in the fractal dimension represents a doubling in the complexity of the structure (Porter et al., 1991).

Consecutive, unbroken series of ultrathin sections, ranging from 15 to 40 in number, were collected and photographed for each endbulb. Due to the large size of individual endbulbs, only relatively small regions of each endbulb were sampled by using serial section analysis. The part of an endbulb visible in ultrathin sections is called a profile. From electron micrographs, the area and perimeter of each labeled profile, and the area and number of the constituent mitochondria were determined by computerized planimetry (SigmaScan, Jandel Scientific, Corte Madera, CA). The above data allowed us to calculate cytoplasmic area (profile area minus mitochondria area), mitochondrial fraction (mitochondrial area divided by cytoplasmic area), and mitochondrial density (number per μm^2). Postsynaptic densities (PSDs) appeared as asymmetric thickenings in the postsynaptic membrane and apposed presynaptic accumulations of synaptic vesicles. The lengths of PSDs were measured, and synaptic vesicles were counted so that their density (number per PSD) could be established.

Ending profiles and PSDs were serially reconstructed from electron micrographs. The resulting "stack" was then rotated and viewed en face by using a computerized imaging system (Eutectics Electronics Inc., Raleigh, NC, or NIH Image Version 1.57 with VoxBlast, VayTek Inc., Fairfield, IA). Reconstructed PSDs were studied as they resided in the postsynaptic membrane, but their sizes

could not be determined because they usually continued further into unexamined sections. Section thickness was estimated by using standard interference reflection colors as the sections floated in the knife trough. The sections were silver in color, more gray than gold, and we estimate their thickness at 75 nm. This value is consistent with our reconstructions, because 14 sections, when rotated 90° and viewed en face span slightly less than 1 μm, as determined by a calibration grid, and 15 sections slightly exceeded 1 μm.

Data from the deaf cats were compared with reanalyzed data from normal cats already available in the lab (raw data from Sento and Ryugo, 1989; Ryugo et al., 1996). All measurements are accompanied by means and standard deviations. Statistical comparisons were conducted by factorial ANOVA (Statview II, Abacus Concepts, Inc., Berkeley, CA), and *P* values are provided where significant differences were detected. Photographic negatives were digitized (Leafscan 45), the contrast and/or exposure adjusted (if necessary), simulating standard darkroom techniques (Adobe Photoshop), and the files printed in high-resolution format (Fuji Pictrography 3000).

RESULTS

The present results are based on examination of the anterior part of the AVCN from 29 normal cats and the nonhearing sides of four DWCs. For our purposes, DWC endbulbs were selected from the cochlear nucleus ipsilateral to cochleae that exhibited the following: no recordable ABR up to the highest stimulus levels and the histologic verification of an absent organ of Corti. The cochleosaccular degeneration associated with the deaf white cats was represented by an absence of hair cells, a missing tunnel of Corti, a rolled-up tectorial membrane, a thinning of the stria vascularis, and the collapse of Reissner's membrane upon the basilar membrane. Spiral ganglion cells were also notably missing throughout Rosenthal's canal, especially in the apex and base (Saada et al., 1995). In contrast, normal endbulbs were collected from hearing cats with N1 thresholds ≤5 dB SPL (Ryugo et al., 1996).

The quantitative light microscopic data were derived from 52 HRP-labeled endbulbs of Held from two DWCs (aged 6 months and 6.5 years) and 66 HRP-labeled endbulbs from normal hearing adult cats. The electron microscopic analyses are based on eight HRP-labeled endbulbs and two unlabeled endbulbs from these same two DWCs, two unlabeled endbulbs from each of two other DWCs (ages 6 and 8 months), and nine HRP-labeled endbulbs from two normal cats (Table 1).

Light microscopic analysis

There were striking differences in structure when we examined endbulbs of Held from the DWCs and compared them with those of normal hearing cats. Normal endbulbs exhibit a complex arborization marked by multiple branches stemming from a single thick trunk (2–3 μm in diameter). Numerous varicosities occur along secondary and tertiary branches with many fine, interconnecting filamentous processes. The endbulb typically contacts up to half the soma of the spherical bushy cell in normal cats (Fig. 2). In contrast, endbulbs of the DWCs are distinctly different. They exhibit a less extensive arborization and the en passant and terminal swellings are fewer in number and larger in size. The arborization of these endings have a diminished meshwork of interconnecting filaments and make smaller somatic contact with the target spherical bushy cells (Fig. 2).

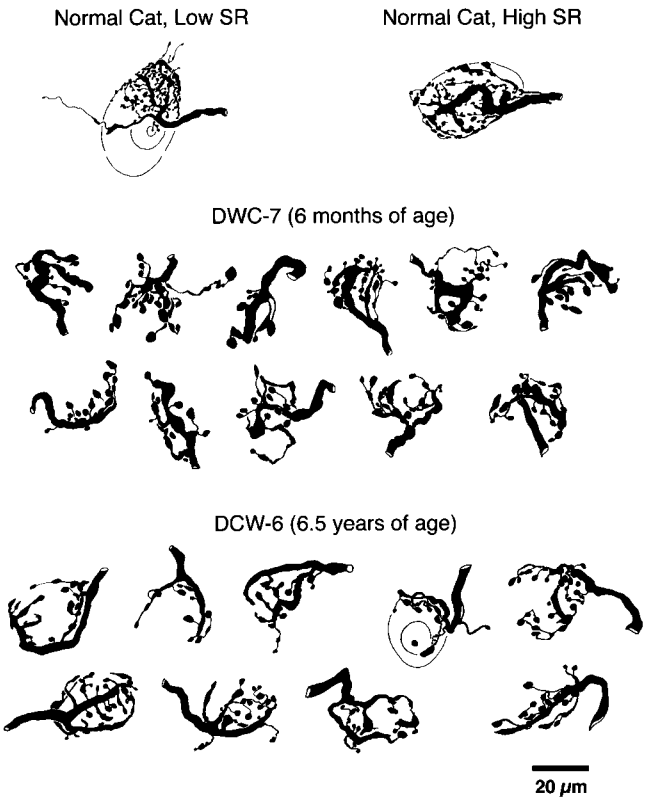

Fig. 2. Drawing tube reconstructions of typical endbulbs analyzed for the present study. The top row illustrates typical endbulbs from low and high spontaneous rate (SR) fibers of normal cats. The middle two rows illustrate endbulbs from a 6-month-old deaf white cat (DWC-7), and the bottom rows are from the 6.5-year-old cat (DWC-6). There is an attenuation of tertiary branching and loss of the fine interconnecting meshwork in endbulbs of the congenitally deaf cats.

Endbulb morphometrics and fractal analysis

Endbulb silhouette area was calculated from the drawing tube reconstructions. Scale bars and individual drawings were digitized, and areas were calculated by using NIH Image. Endbulb area is smaller in DWCs (171.8 ± 61 μm^2) compared with normal cats (390.1 ± 177 μm^2, $P < 0.0001$). Normal endbulbs of low SR fibers are typically smaller (288.1 ± 62.2 μm^2) than those of high SR fibers (499.0 ± 170.1 μm^2, $P < 0.05$). These endbulbs were smaller because their arborizations appeared stunted. The validity of this assessment was confirmed by fractal analysis.

Fractal analysis

Fractal analysis is a useful tool for quantifying structural complexity (Mandelbrot, 1982; Smith et al., 1989), and its application to neuronal morphology has been previously used (Fernandez et al., 1994; Panico and Sterling, 1995; Aboujaoude et al., 1996). There was no difference in fractal dimension values between the 6-month-old DWC (1.278 ± 0.04) and the 6.5-year-old DWC (1.284 ± 0.05, $P < 0.67$). There was, however, a difference when

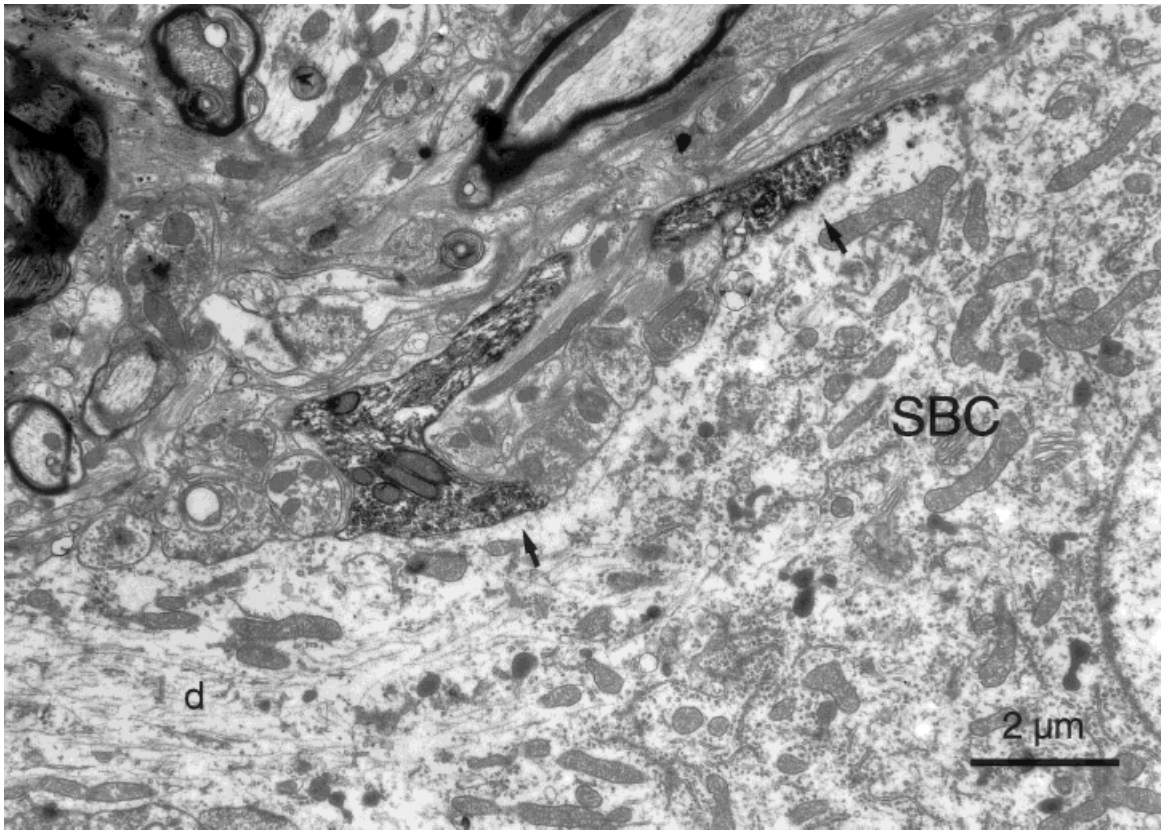

Fig. 3. Electron micrograph illustrating HRP-labeled endbulb profiles (arrows) in contact with the cell body and proximal dendrite (d) of a spherical bushy cell (SBC). The horseradish peroxidase (HRP) reaction product clearly distinguishes labeled from unlabeled structures. Note that this cell is also postsynaptic to small bouton endings.

comparing the DWC endbulbs with the fractal index of normal cat endbulbs (1.412 ± 0.52, $P < 0.0001$). These fractal values provide a quantitative measure for the subjective impression gleaned from the light microscopic appearance of endbulbs among the different cats (Fig. 2).

Ultrastructural characteristics

Labeled endbulbs can be reliably distinguished in the electron microscope due to the presence of HRP reaction product within the cytoplasm (Fig. 3). These endbulbs make contact with the somata of spherical bushy cells and the shafts of their primary dendrites. The postsynaptic neurons are identifiable by virtue of their physical relationship to endbulbs, their round-to-oval cell body, and abundant cytoplasmic Nissl bodies. The nucleus is round, pale-staining, and centrally placed, but unlike normal cats, spherical bushy cells of the DWCs do not always exhibit the prominent perinuclear Nissl cap.

At higher magnifications, structural features exhibited by these endings form a constellation of specializations representing the functional synapse, e.g., criteria of Cant and Morest, 1979; Fekete et al., 1984. In normal hearing cats, these features include the presence of clear, round synaptic vesicles, numerous mitochondria, and a prominent thickening (known as the PSD) along the postsynaptic membrane. Presynaptic endings form a broad apposition that abuts the spherical bushy cell, and within a typical cross section, one or more PSDs are usually present. PSDs typically bulge into the presynaptic endbulb (Fig. 4, top). In DWCs, however, this synaptic interface is distinctly different. The postsynaptic bulge is much less apparent, there is a pronounced membranous fuzz along the presynaptic membrane, there are fewer synaptic vesicles distributed within the ending, and the PSDs are characteristically long especially when compared with those of normal cats (Figs. 4, 5).

Striking reductions in the number of synaptic vesicles were observed with respect to deafness and duration of deafness. The number of synaptic vesicles was counted from electron micrographs at a printed magnification of ×70,000. Only complete profiles were examined. Vesicle number was analyzed with respect to PSD per profile and found to differ between normal and deaf cats ($P < 0.0001$). The DWC profiles had 51.1 ± 67.1, compared with normal profiles, which had 70.9 ± 79.4 synaptic vesicles. These data emphasize that vesicle number is diminished in DWCs.

In all tissue sections, we observed large, unlabeled endings that contained large, round synaptic vesicles and were associated with prominent asymmetric membrane thickenings (Fig. 6A). These endings were found contacting the somata of spherical bushy cells and exhibited intracellular morphology resembling what was found in labeled endbulbs. Thus, these endings were identified as

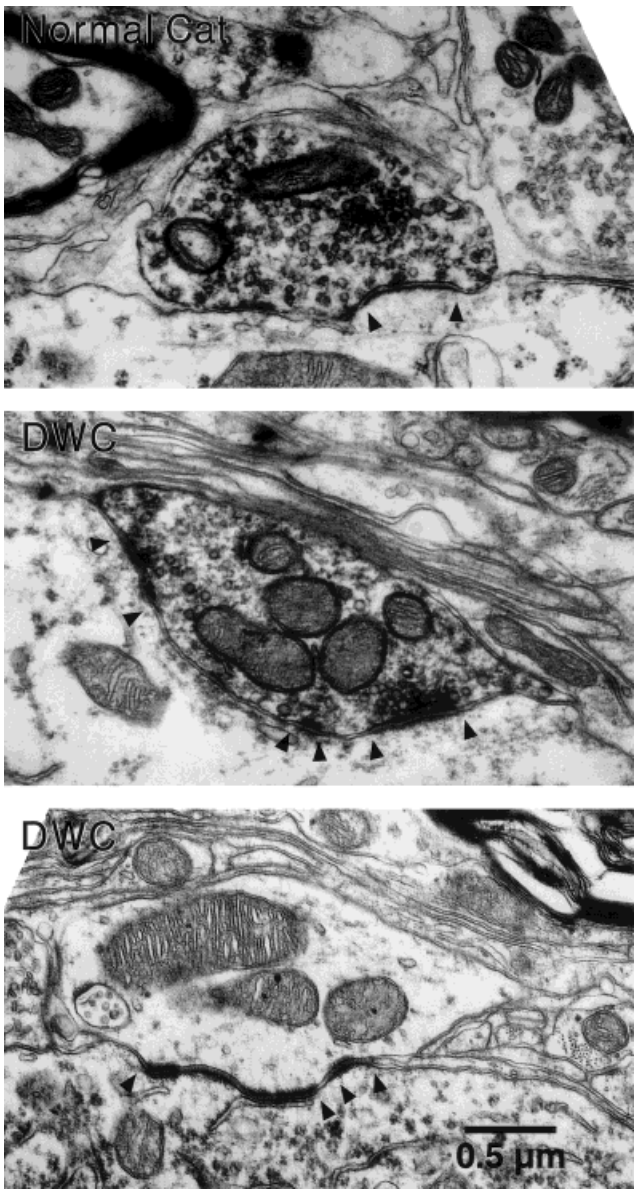

Fig. 4. Electron micrograph of endbulb profiles that contact spherical bushy cells. **Top:** Taken from a normal cat, where an HRP-labeled endbulb makes a synapse characteristic of myelinated auditory nerve fibers. The profile is filled with clear, round synaptic vesicles, there is a well-defined postsynaptic density (PSD; between the arrowheads), and the postsynaptic membrane bulges out slightly into the terminal. In contrast, endbulb profiles from DWCs are strikingly different in appearance. **Middle:** Illustrates HRP-labeled endbulb taken from a young DWC (6 months of age). Note that synaptic vesicles are clustered near PSDs rather than being distributed uniformly throughout and that their number is smaller. Also, the ending itself has indented the postsynaptic membrane. **Bottom:** A representative unlabeled ending from the 6.5-year-old deaf cat. This ending indents the somatic membrane, is nearly devoid of synaptic vesicles, and exhibits long and prominent pre- and postsynaptic densities. The enhanced membrane densities are the most salient features of DWC synapses, and they were evident on the deaf side of all cats older than 6 months of age.

endbulbs. The endbulbs of DWCs exhibited a wide range in synaptic vesicle density, some approaching near normal numbers (Fig. 6A) and others much fewer (Fig. 6B). Some of the primary endings contained distinctly large mitochondria and practically no synaptic vesicles (Figs. 6C, 7). Although these mitochondria were not swollen and did not contain vacuoles, perhaps their presence was indicative of some other degenerative process (e.g., Gray and Guillery, 1966).

In both normal and deaf white cats, there were small bouton endings in addition to large endbulbs which formed synaptic contacts with the cell bodies of spherical bushy cells. Bouton endings, as determined by serial section analysis, are somewhat spherical structures, ranging from 1 to 3 μm in diameter and filled with synaptic vesicles. The most common class of bouton typically contained synaptic vesicles of all shapes with many of them extremely flattened (Fig. 7). Less common but still evident are boutons containing a complement of pleomorphic synaptic vesicles, few of which are flattened. These boutons are not of primary origin (Cant and Morest, 1979), and in DWCs, the synaptic vesicle content and symmetric PSD shape had a normal appearance (Fig. 7). We did not attempt to determine whether there was a loss of these types of endings along the bushy cell body. The other class of boutons was clearly cochlear in origin by virtue of their round synaptic vesicles and asymmetric PSDs, and in DWCs, these exhibited the same abnormal constellation of characteristics found in endbulbs (Fig. 7).

Mitochondria. Mitochondria are readily identifiable organelles and obviously important for maintaining the metabolic activity in neurons. We hypothesized that deafness could alter neuronal metabolism in auditory neurons because of the decrease in auditory-evoked activity, and that such a change might be evident in mitochondrial structure. For the most part, however, mitochondria appeared normal for both hearing and deaf cats except in a subpopulation of endings from the DWCs in which mitochondria were remarkably hypertrophied. The mitochondrial cristae exhibited the same luminal diameter and spacing as most normal mitochondria (Figs. 6C, 7) and so gave the appearance of normal but very large structures.

The fraction of profile area occupied by mitochondria differed between the normal and DWCs. It was greater in the DWCs (16.8 $\pm$ 10.7%) than in the normal cats (12.4 $\pm$ 11.2%, $P < 0.01$), but there was no difference between the DWCs of different ages. These data indicate a greater mitochondria density in the population of endbulbs from DWCs when compared with normals, perhaps because DWC ending volume is smaller.

Synapses. Endbulb synapses are found along the cell body or proximal dendrite of spherical bushy cells (Fig. 3). We verified through serial section analysis that, in addition to these axosomatic synapses, there are also synapses onto dendrites in the neuropil. These axodendritic synapses occurred in two arrangements: Endbulb collaterals synapse upon dendrites in the neuropil (Fig. 8A), or axodendritic synapses arise on the side opposite the axosomatic synapses (Fig. 8B). Dendrites were identified by virtue of their thin caliber and a lack of Golgi apparatus and ribosomes. These axodendritic relationships, which have been previously reported in the normal cat (Lenn and Reese, 1966; Cant and Morest, 1979; Ryugo and Sento, 1991), comprised 17 $\pm$ 5.2% of the synapses analyzed in the DWCs, and their frequency was not statistically different ($P < 0.22$) from that of normal high SR endbulbs (13.6 $\pm$ 2.5%, Ryugo et al., 1996).

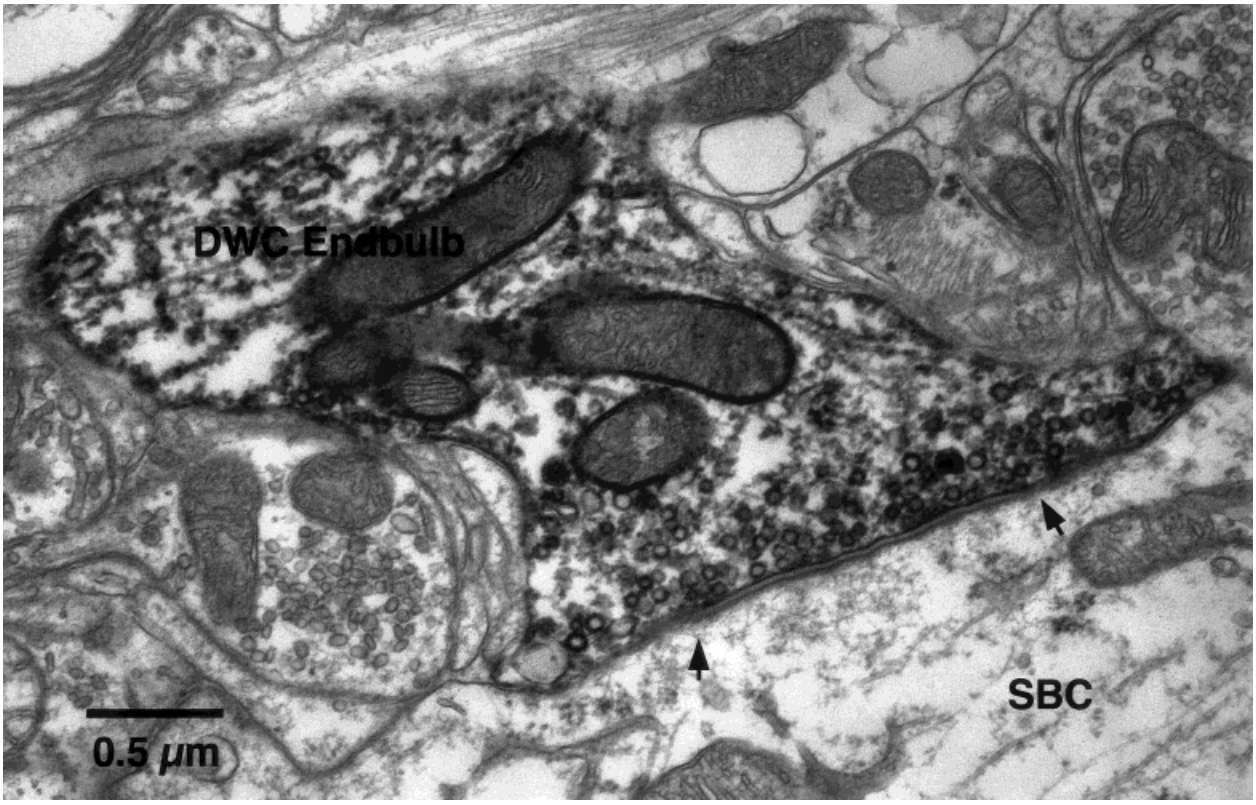

Fig. 5. Electron micrograph of HRP-labeled endbulb profile from the 6-month-old DWC. Note the diminished number of synaptic vesicles and the length of the pronounced pre- and postsynaptic densities (bounded by arrows). SBC, spherical bushy cell.

The synapses of DWCs are strikingly different in appearance from those of normal cats. Specifically, the PSDs are thicker, longer, and without the distinctive outward curvature that typically characterizes PSDs of hearing cats. Instead, the axosomatic endings often appear to be embedded in the cell body (Figs. 4, 8B). In a random sample of endbulb profiles, the mean lengths of axosomatic PSDs from the DWCs was 0.32 ± 0.21 μm, n = 473. This value is nearly 50% greater ($P < 0.0001$) than that of endings from normal hearing cats (0.22 ± 0.23 μm, n = 200). In contrast, the mean length of axodendritic PSDs of the DWCs was 0.26 ± 0.19 μm, n = 108, which is identical to that of normal cats.

The PSDs of endbulbs from normal cats have, on average, significant convex curvature where the PSD of the spherical bushy cell membrane bulges into the presynaptic ending (Ibata and Pappas, 1976; Gulley et al., 1978; Cant and Morest, 1979). Furthermore, there is a higher degree of curvature for high SR fibers than low SR fibers (Ryugo et al., 1996). The endbulbs of the DWCs in this study exhibited no systematic curvature of the PSDs. Individual PSDs could exhibit concave or convex curvature, and some had both (Figs. 5, 6), but many were simply flat (Fig. 5).

There were approximately twice as many PSDs per ending profile in DWCs compared with the normal population. There were 2.74 ± 1.79 PSDs per profile in the DWCs and 1.43 ± 1.28 PSDs per profile in normal cats. This kind of analysis in random sections implies that there is a significantly greater number of synapses in endbulbs of DWCs compared with normal cats ($P < 0.001$).

Active zone reconstructions. The idea that DWCs had more and larger synapses prompted us to reconstruct synapses in three dimensions through serial sections. We collected and analyzed unbroken strings of 15–40 serial ultrathin sections through random regions in each of the 14 different endbulbs. PSD and profile apposition areas were analyzed by aligning serial ultrathin sections, tracing them and a calibration grid into a computer-assisted reconstruction program, and rotating the resultant images 90° to be viewed en face. These en face reconstructions revealed a marked difference between synapses of DWCs and normals. First, we learned that DWC endbulbs did not have twice as many active zones as was suggested by random section analysis, but rather, exhibited large, irregularly shaped active zones that weaved around the surface of the postsynaptic cell (Fig. 9). This shape is in sharp contrast to the small (0.14 ± 0.06 μm^2), round-to-oval PSDs observed in normal endings. The mean PSD area for the DWCs is 0.24 ± 0.36 μm^2, although this value is an underestimation because many of the active zones continued beyond the last section analyzed. These results indicate that DWC synapses are on average approximately twice as large as those (0.14 ± 0.06 μm^2) of normal cats. Second, we discovered that synaptic characteristics (e.g., PSD size, synaptic vesicle distribution, or mitochondria volume fraction) did not differ among our DWCs with respect to age of the animal. That is, by 6 months of age, it appears that synaptic abnormalities in the endbulbs of DWCs have stabilized.

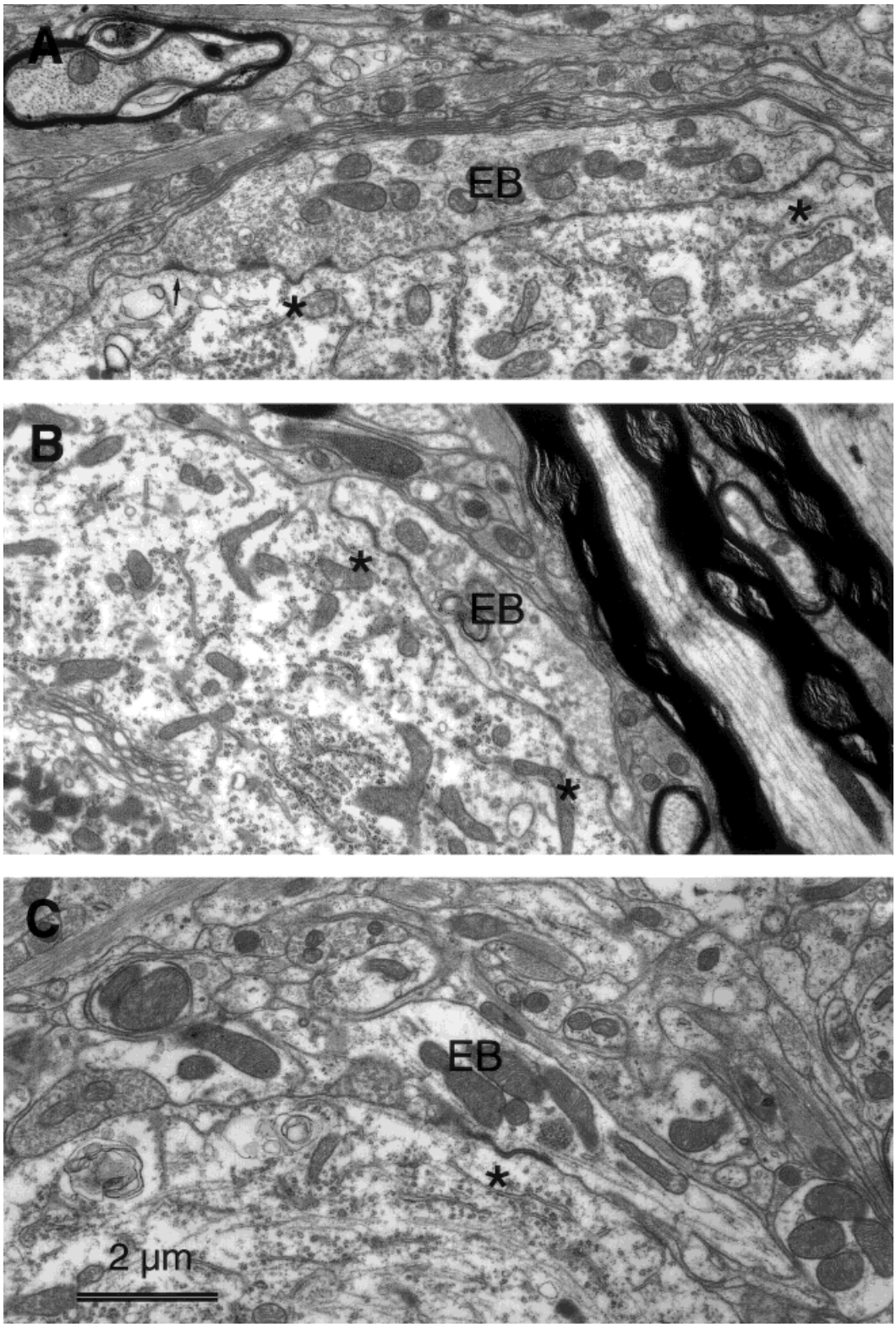

Fig. 6. Electron micrographs of unlabeled endbulb processes (EB) from deaf white cats illustrating not only a variety in appearance but also a constancy in large PSDs. **A:** This process exhibits many clear, round vesicles and forms prominent asymmetric synapses. Most of the endbulb processes in the DWCs, whether labeled or unlabeled, resemble this profile. A small PSD (arrow) and two large PSDs (*) are indicated. **B:** This endbulb contains vesicles having the same size and shape as those of normal endbulbs, but there are fewer of them. The ending forms two long and prominent PSDs (*). **C:** This process appears different from other endbulbs by virtue of its greatly enlarged mitochondria but is similar by its relative absence of synaptic vesicles and enlarged PSDs (*). Endbulbs having these features were found in DWCs of all ages studied (6 months to 6.5 years).

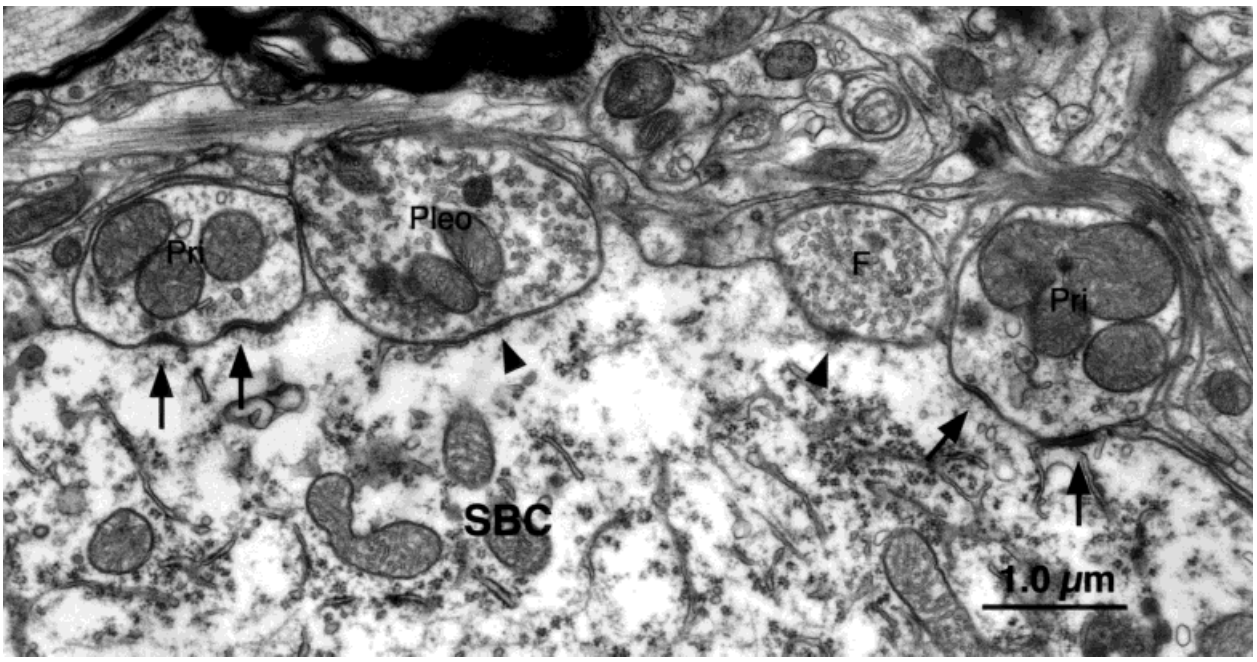

Fig. 7. Electron micrograph of unlabeled bouton endings in the 6.5-year-old DWC. Abnormal primary endings (Pri) contain enlarged mitochondria, few synaptic vesicles, and prominent but irregularly shaped PSDs (arrows). Note also the bouton profiles containing pleomorphic (Pleo) and flattened (F) synaptic vesicles with a symmetric PSD (arrowheads). The nonprimary endings in the DWCs had a normal appearance.

Estimated total area of synapses. The number of axosomatic synapses was calculated for each endbulb by assuming that synapse density was uniform across the entire endbulb. This assumption seems appropriate because synapse density was uniform for the regions reconstructed. The number of PSDs per unit of apposition area was multiplied by the endbulb silhouette area as determined via light microscopy, yielding an estimate of the number of PSDs for the entire endbulb. We also assume that apposition area approximates endbulb silhouette area. By this means, we estimate that there are 261.9 ± 158.0 synapses per endbulb for the DWCs. By comparison, it has been estimated that there are 461 ± 135 synapses for low SR endbulbs and 1,737 ± 650 synapses for high SR endbulbs in normal cats (Ryugo et al., 1996). Multiplying the total number of synapses per endbulb by the average area of individual synapses yields the total synaptic area for each endbulb. This value is 69.5 ± 41.7 μm^2 for the DWCs, compared with 114.9 ± 74.9 μm^2 for endbulbs of normal cats ($P < 0.0001$).

DISCUSSION

The present study examined endbulbs of Held and their synaptic relationship with spherical bushy cells in the AVCN of congenitally deaf cats. It is well documented that neurons of the cochlear nucleus shrink when they are deprived of normal cochlear input as in the case of congenital deafness (West and Harrison, 1973; Larsen and Kirchhoff, 1992) or cochlear ablation (Powell and Erulkar, 1962; Trune, 1982; Born and Rubel, 1985). These transneuronal effects in the auditory system are analogous to what has been reported for other sensory systems (e.g., Wiesel and Hubel, 1963; Benson et al., 1984; Durham and Woolsey, 1984). Our study extended what is known about the effects of congenital deafness in the cochlear nucleus by examining the ultrastructural characteristics of pre- and postsynaptic elements in subjects after 6 months and up to 6.5 years of deafness. Compared with normal hearing cats, endbulbs of DWCs are structurally abnormal, typified by reduced numbers of synaptic vesicles and PSDs that are strikingly hypertrophic (Table 2).

Three types of axosomatic endings in DWCs are seen with respect to vesicle shape: profiles of variable shapes with round, clear vesicles; small boutons with flat vesicles; and small boutons with pleomorphic vesicles. Each of these endings types is represented in the AVCN of normal cats (Ibata and Pappas, 1976; Cant and Morest, 1979; Treeck and Pirsig, 1979). There was no obvious difference in distribution of the three types of endings contacting the surface of the spherical bushy cell, except for the diminished surface contact by endbulbs in the adult DWC. Likewise, those boutons with flat or pleomorphic vesicles appeared normal with respect to their size, shape, vesicle or mitochondrial content, and PSD characteristics. There is a differential expression of synaptic anomalies, which are obvious in the primary endings but not in the nonprimary endings. Our failure to detect change in nonprimary endings implies that any induced pathology is too subtle for our methods, or that the endings are too removed from the degenerative source to be affected. The data do suggest that the abnormalities in primary endings are most likely a result of the cochlear pathology.

Because DWCs differ genotypically from normal cats, it is also possible that the synaptic differences we observed arise from genes other than those controlling cochlear function. That is, perhaps synapses in nonauditory structures of DWCs are also abnormal. We did not process the

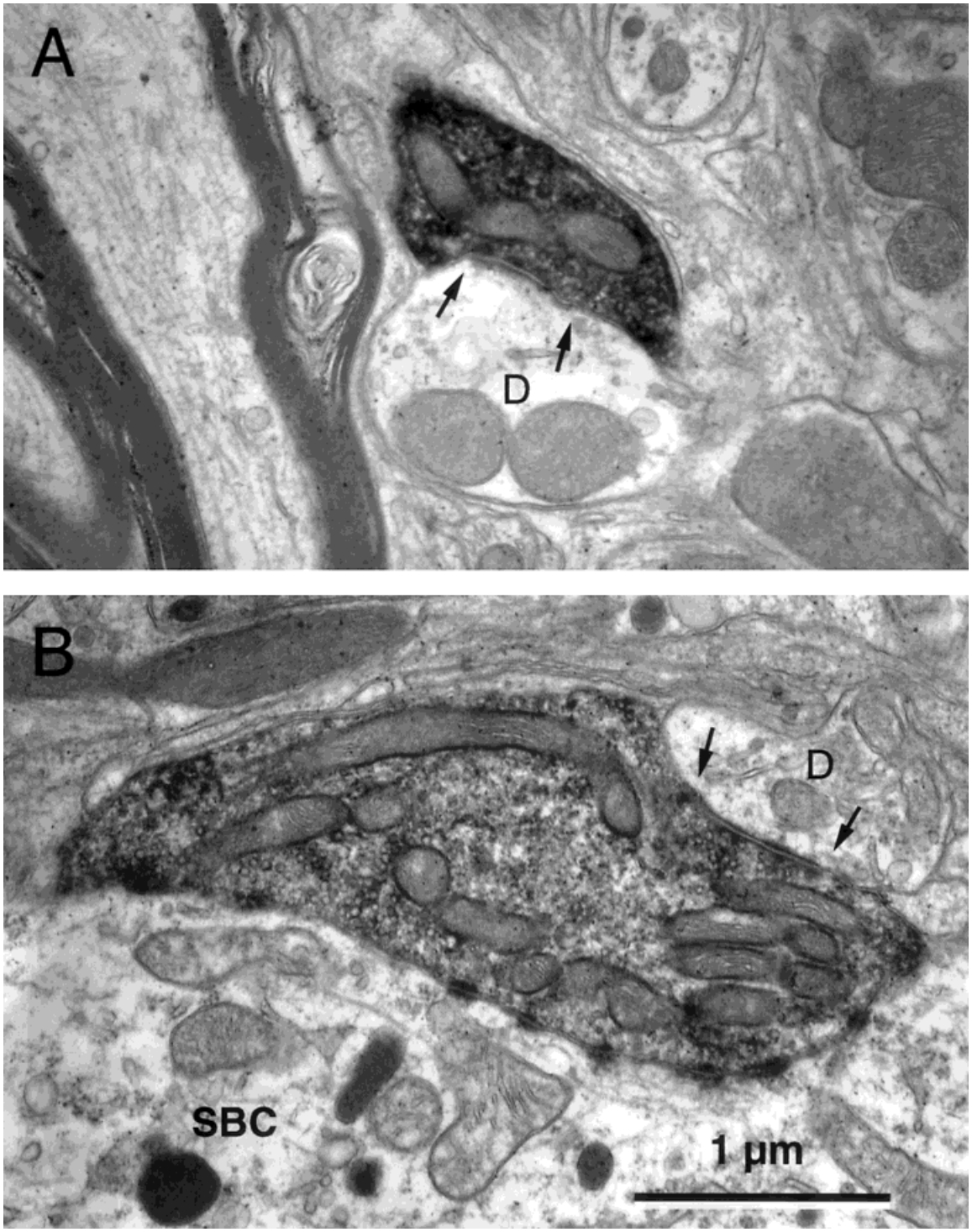

Fig. 8. Electron micrographs of HRP-labeled endbulb profiles of the 6-month-old DWC. **A:** This axodendritic synapse arises from a short collateral of the endbulb and contacts a dendrite in the neuropil. Note the prominent PSD (flanked by arrows) with a dendrite of unknown origin. **B:** This endbulb profile is in contact with both the soma of a spherical bushy cell (SBC) and a dendrite (D). The labeled process is filled with synaptic vesicles and partially invades the soma. The endbulbs of DWCs expressed axodendritic and axosomatic synapses, similar to what is observed in normal hearing cats.

entire brain of the deaf white cats for electron microscopy, so only cerebellar tissue overlying the cochlear nucleus was available for examination. This tissue, however, is from the floccular lobe and part of the vestibulocerebellum, which was affected by the pathology. The basic synaptic components and organization were present (Palay and

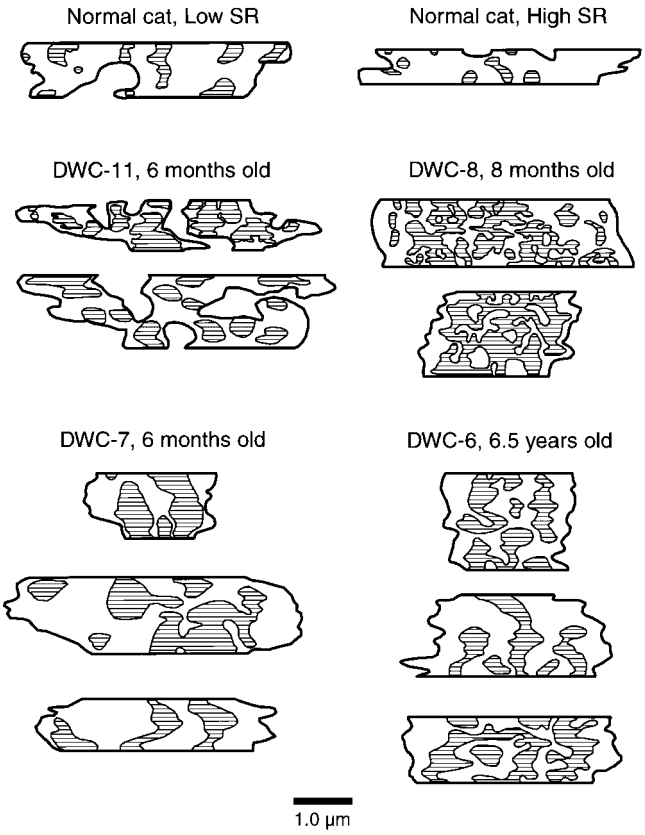

Fig. 9. Representative appearance of synaptic active zones (horizontal stripes) and apposition areas (clear) when reconstructed via serial ultrathin sections and viewed en face. **Top:** View of PSDs from low and high spontaneous rate auditory nerve fibers from normal cats. Note that the PSDs are relatively small and mostly ovoid or mildly irregular in shape. **Bottom:** PSDs from the deaf white cats. Note that these PSDs are large and irregular in shape. Because the size of PSDs is stable after 6 months, we infer that the "upregulation" of PSDs occurs during an earlier postnatal period.

TABLE 2. Summary of Endbulb Data, Comparing DWCs With Normal Cats

Structural features	DWCs[1]	Normal cats[2]	*P* values
Number of cats	4	33	
Number of endbulbs	52 (14 for EM)	67 (9 for EM)	
Endbulb silhouette area (μm²)	171.8 ± 61 (n = 52)	390.3 ± 177 (n = 67)	<0.0001
Endbulb fractal dimension	1.28 ± 0.05 (n = 52)	1.41 ± 0.05 (n = 67)	<0.0001
Number of profiles analyzed	435	209	
Mitochondria volume fraction (%)	16.8 ± 10.7	12.4 ± 9.4	<0.01
Number of mitochondria per μm²	2.80 ± 1.86	2.11 ± 2.03	<0.01
Number of PSDs per profile	2.73 ± 1.73	1.43 ± 1.28	<0.01
Number of synaptic vesicles per PSD	73.9 ± 82.6	68.6 ± 34.8	<0.01
PSD size (μm²)	0.24 ± 0.36 (n = 59)	0.14 ± 0.06 (n = 139)	<0.01

[1]Light microscopic analysis of labeled endbulbs was from one 6-month-old deaf whitecat and one 6.5-year-old deaf white cat. EM analysis included all 4 DWCs. ANOVA statistics were applied to these data. Values are means ± SD.
[2]Data from high (n = 40) and low (n = 27) SR fibers are combined for light microscopy. Reanalyzed from Sento and Ryugo, 1989 and Ryugo et al., 1996.
DCW, deaf white cat; PSD, postsynaptic density.

Chan-Palay, 1974) but we could not determine unambiguously if there were systematic differences between the synapses of DWCs and normals. In fact, such an endeavor is well beyond the scope of this presentation. For the present, we shall argue that there is not some sort of global brain pathology because these deaf cats had normal gait and posture, regular appetite and reproductive behavior, and appropriate responses to petting, visual stimuli, and nociception.

Morphometric analysis: Form factor and fractals

Light microscopic morphometry indicated less structural complexity of endbulbs in DWCs as well as diminished area of contact compared with that of normal cats. That is, endbulbs of DWCs exhibited less tertiary branching, and we interpret this feature of morphology to reflect diminished neural activity. Fractal analysis provided a numerical index that correlated the atrophic, light microscopic appearance of endbulbs to the relative physiologic inactivity of the primary fibers. We hypothesized that DWCs, which we originally expected to have no activity in their auditory nerves, would exhibit endbulbs that resembled low SR endbulbs in appearance. To be sure, endbulbs of DWCs were structurally abnormal but did not resemble endbulbs of normal low SR fibers. Fractal values were consistent with diminished complexity of endbulb shape in protracted deafness, as hypothesized. A major complication for our hypothesis was that not all auditory nerve fibers of the DWC were silent, and some exhibited spontaneous activity up to 100 spikes per second (Saada et al., 1995). It could be that silent fibers would have endbulbs that appeared atrophic, whereas that small population of active fibers would have endbulbs that appeared normal. On the other hand, endbulb shape might be determined by more than spontaneous spike activity, where sound-evoked, patterned activity is the essential component to normal maintenance of endbulb morphology. Intracellular staining of silent versus spontaneously active auditory nerve fibers of DWCs is needed to assess unequivocally the role of spike activity in ending shape and synapse size. An additional question is whether electrical stimulation can produce the pattern of neural activity needed to maintain synapse structure and function.

Synaptic characteristics

The synaptic active zone is identifiable by the presynaptic accumulation of vesicles in close proximity to a postsynaptic membrane thickening (PSD) and represents the release site for neurotransmitter. The typical PSD has the shape of an ovoid or mildly irregular disk. Although the basic structural features of synapses appear to be conserved in DWCs, abnormalities are also evident. Already by 6 months of age, the postsynaptic densities in the DWCs are thickened and have formed expansive yet irregular serpentine structure along the surface of the postsynaptic neuron. This arrangement of the PSDs appeared fully developed at this age, and we could not discern any additional changes in the older DWCs. Where inactivity produces an increase in PSD size (present report), excessive stimulation is reported to produce a reduction (Rees et al., 1985). These data are mutually consistent with the idea that intrinsic structure of the PSD matrix is influenced by levels of activity (Greenough et al., 1978; Bailey and Chen, 1983; Desmond and Levy, 1986).

Why PSDs spread and thicken at inactive synapses is unknown. Functional recovery may depend on such compensations to confer greater efficacy for the remaining neuronal elements (Hillman and Chen, 1985). In the case of DWC endbulbs, remodeling of pre- and postsynaptic

membrane specializations may represent a mechanism for optimizing synaptic transmission in the face of reduced transmitter release. Because neurotransmitter receptors reside within the PSD (Seitanidou et al., 1988; Flucher and Daniels, 1989; Nusser et al., 1994), the growth of PSDs could reflect an "upregulation" of receptor proteins such that the postsynaptic cells could detect even minute amounts of transmitter release.

Functional significance

Endbulbs of Held are large axosomatic endings located in the rostral AVCN and arise from type I spiral ganglion neurons (Held, 1893; Ramón y Cajal, 1909; Lorente de Nó, 1981; Ryugo and Fekete, 1982). Each inner hair cell has a direct one-to-one line to a spherical bushy cell of the cochlear nucleus by way of an endbulb of Held (Sento and Ryugo, 1989). Because the cochlear nucleus gives rise to the central ascending auditory pathways, alterations at this nucleus are expected to have consequences throughout the neuraxis (e.g., Moore, 1990). Although the functional state of the synapse was not tested by this study, pathology was inferred by the presence of diminished synaptic vesicle density, reduced mitochondrial volume fraction, and hypertrophy of pre- and postsynaptic membrane thickenings.

The endbulb of Held is one of the largest synaptic endings in the central nervous system (Ramón y Cajal, 1909; Lorente de Nó, 1981). Furthermore, it is estimated that a single endbulb has as many as 1,700 active zones or release sites (Ryugo et al., 1996). These structural characteristics are consistent with the idea that endbulbs have high-fidelity synaptic transmission where every presynaptic event triggers a postsynaptic response (Pfeiffer, 1966; Molnar and Pfeiffer, 1968; Sullivan and Konishi, 1984). The significance of this "fail-safe" synapse is that acoustic stimuli in the environment are tightly coupled in the temporal domain to neural responses. Thus, the endbulb-bushy cell pathway is not only integral to the processing of timing cues for sound localization but also key to analyzing the temporal properties of speech sounds, such as formant transitions, prosody, and phoneme duration. The successful processing of these kinds of sounds is critical to effective speech recognition, and the endbulb is an invaluable component.

Clinical considerations

There is significance for understanding the functional capabilities of auditory synapses in congenital deafness. If the synaptic efficacy of endbulbs is compromised, crucial information will be lost at this interface especially with respect to temporal processing. Our data are pertinent to reports that cochlear implants have superior benefit for individuals who become deaf postlingually compared with those who become deaf prelingually (Waltzman et al., 1992; Waltzman et al., 1994; Gantz et al., 1994). One interpretation of this age-related phenomenon is that early-onset deafness initiates alterations in the synaptic connections of the central auditory system during the period when the system is being formed. Deaf children have received cochlear implants, and preliminary data concerning this intervention practice indicate that younger recipients ultimately achieve higher levels of speech recognition (Waltzman et al., 1994). One implication relating our observations to clinical data is that beginning with the cochlea, progressive changes along the auditory pathways render acoustic stimuli less meaningful over time, especially as duration of deafness increases. If implantation is performed during the period when functional connections are being formed, the deleterious effects of deafness on the central auditory system might be ameliorated, and the development of aural and oral language may be facilitated. After this critical period, however, the resulting deafness-induced synaptic changes may impair the processing of prosthetic input.

During the early history of cochlear implant development, it was assumed that restored input by itself could activate the system and replace previously lost auditory information. This assumption, however, is probably not valid. In addition to our data, recent anatomical observations of human cochlear nuclei from profoundly deaf donors revealed a diminution of neurons in the ventral cochlear nucleus (Seldon and Clark, 1991; Moore et al., 1994). The most profound effect was seen in cases of congenital dysmorphia (Scheibe deformities) compared with acquired hearing loss in which duration of deafness was equally prolonged (Moore et al., 1994). If connections within the auditory pathway slowly change as a consequence of early-onset deafness, the pathway may no longer be capable of encoding simulated inputs from a prosthetic device. This deficiency would be particularly evident when processing sounds as complex as speech, thereby reducing the usefulness of signals from cochlear implants. The task remains a problem of knowing the processing capabilities of the remaining neural structures following prolonged periods of early-onset deafness and the time frame during which deafness-induced change occurs.

ACKNOWLEDGMENTS

The authors gratefully thank Brian T. Rosenbaum, Edward S. Aboujaoude, Ahmed A. Saada, and Rachael Urik for technical assistance, and Dr. Peter Sterling for the suggestion to apply fractal analysis on endbulb shape. This work was supported by research grant number 5 RO1 DC00232 to D.K.R. and a CIDA grant to J.K.N. from the National Institute of Deafness and Other Communication Disorders, National Institutes of Health.

LITERATURE CITED

Aboujaoude, E.S., J.K. Niparko, and D.K. Ryugo (1996) Fractal analysis of endbulbs of Held in cats. ARO Abstr. *19:*171.

Bailey, C.H., and M. Chen (1983) Morphological basis of long-term habituation and sensitization in *Aplysia*. Science *220:*91–93.

Bakin, J.S., and N.M. Weinberger (1990) Classical conditioning induces CS-specific receptive field plasticity in the auditory cortex of the guinea pig. Brain Res. *536:*271–286.

Benes, F.M., T.N. Parks, and E.W Rubel (1977) Rapid dendritic atrophy following deafferentation: An EM morphometric analysis. Brain Res. *122:*1–13.

Benson, T.W., D.K. Ryugo, and J.W. Hinds (1984) Effects of sensory deprivation on the developing mouse olfactory system: A light and electron microscopic, morphometric analysis. J. Neurosci. *4:*638–653.

Bergsma, D., and K. Brown (1971) White fur, blue eyes, and deafness in the domestic cat. J. Hered. *62:*171–185.

Born, D.E., and E.W. Rubel (1985) Afferent influences on brain stem auditory nuclei of the chicken: Neuron number and size following cochlea removal. J. Comp. Neurol. *231:*435–445.

Born, D.E., D. Durham, and E.W. Rubel (1991) Afferent influences on brainstem auditory nuclei of the chick: Nucleus magnocellularis neuronal activity following cochlea removal. Brain Res. *557:*37–47.

Bosher, S.K., and C.S. Hallpike (1965) Observations on the histological features, development and pathogenesis of the inner ear degeneration of the deaf white cat. Proc. R. Soc. Lond. B *162:*147–170.

Brighton, P., R. Ramesar, I. Winship, D. Viljoen, J. Greenberg, K. Young, D. Curtis, and S. Sellars (1991) Hearing impairment and pigmentary disturbance. Ann. NY Acad. Sci. *630:*152–166.

Cant, N.B., and D.K. Morest (1979) Organization of the neurons in the anterior division of the anteroventral cochlear nucleus of the cat. Light-microscopic observations. Neuroscience *4:*1909–1923.

Desmond, N.L., and W.B. Levy (1986) Changes in the postsynaptic density with long-term potentiation in the dentate gyrus. J. Comp. Neurol. *253:*476–482.

Deitch, J.S., and E.W. Rubel (1984) Afferent influences on brain stem auditory nuclei of the chicken: Time course and specificity of dendritic atrophy following deafferentation. J. Comp. Neurol. *229:*66–79.

Deitch, J.S., and E.W. Rubel (1989a) Changes in neuronal cell bodies in *N. laminaris* during deafferentation-induced dendritic atrophy. J. Comp. Neurol. *281:*259–268.

Deitch, J.S., and E.W. Rubel (1989b) Rapid changes in ultrastructure during deafferentation-induced dendritic atrophy. J. Comp. Neurol. *281:*234–258.

Deol, M.S. (1970) The relationship between abnormalities of pigmentation and of the inner ear. Proc. R. Soc. Lond. *175:*201–217.

Durham, D., and T.A. Woolsey (1984) Effects of neonatal whisker lesions on mouse central trigeminal pathways. J. Comp. Neurol. *223:*424–447.

Fekete, D.M., E.M. Rouiller, M.C. Liberman, and D.K. Ryugo (1984) The central projections of intracellularly labeled auditory nerve fibers in cats. J. Comp. Neurol. *229:*432–450.

Fernandez, E., W.D. Eldred, J. Ammermüller, A. Block, W. Von Bloh, and H. Kolb (1994) Complexity and scaling properties of amacrine, ganglion, horizontal, and bipolar cells in the turtle retina. J. Comp. Neurol. *347:*397–408.

Flucher, B.E., and M.P. Daniels (1989) Distribution of Na^+ channels and ankyrin in neuromuscular junctions is complementary to that of acetylcholine receptors and the 43 KD protein. Neuron *3:*163–175.

Gantz, B., R. Tyler, G. Woodworth, N. Tye-Murray, and H. Fryauf-Bertschy (1994) Results of multichannel cochlear implants in congenital and acquired prelingual deafness in children: Five year follow up. Am. J. Otol. *15:*1–8.

Gray, E.G., and R.W. Guillery (1966) Synaptic morphology in the normal and degenerating nervous system. Int. Rev. Cytol. *19:*111–182.

Greenough, W.T., R.W. West, and T.J. DeVoodg (1978) Subsynaptic plate perforations: Changes with age and experience in the rat. Science *202:*1096–1098.

Gulley, R.L., D.M.D. Landis, and T.S. Reese (1978) Internal organization of membranes at endbulbs of Held in the anteroventral cochlear nucleus. J. Comp. Neurol. *180:*707–742.

Hashisaki, G.T., and E.W. Rubel (1989) Effects of unilateral cochlea removal on anteroventral cochlear nucleus neurons in developing gerbils. J. Comp. Neurol. *283:*5–73.

Held, H. (1893) Die centrale gehörleitung. Arch. Physiol. Anat. 201–248.

Hillman, D.E., and S. Chen (1985) Plasticity in the size of presynaptic and postsynaptic membrane specializations. In C.W. Cotman (ed): Synaptic Plasticity. New York: Guilford Press, pp. 39–75.

Ibata, Y., and G.D. Pappas (1976) The fine structure of synapses in relation to the large spherical neurons in the anterior ventral cochlear (sic) of the cat. J. Neurocytol. *5:*395–406.

Larsen, S.A., and T.M. Kirchhoff (1992) Anatomical evidence of plasticity in the cochlear nuclei of deaf white cats. Exp. Neurol. *115:*151–157.

Lenn, N.J., and T.S. Reese (1966) The fine structure of nerve endings in the nucleus of the trapezoid body and the ventral cochlear nucleus. Am. J. Anat. *118:*375–390.

Lesperance, M.M., R.H. Helfert, and R.A. Altschuler (1995) Deafness induced cell size changes in rostral AVCN of the guinea pig. Hear. Res. *86:*77–81.

Lorente de Nó, R. (1981) The Primary Acoustic Nuclei. New York: Raven Press.

Lustig, L.R., P.A. Leake, R.L. Snyder, and S.J. Rebscher (1994) Changes in the cat cochlear nucleus following neonatal deafening and chronic intracochlear electrical stimulation. Hear. Res. *74:*29–37.

Mair, I.W. (1973) Hereditary deafness in the white cat. Acta. Otolaryngol. *314:*1–48.

Mandelbrot, B.B. (1982) The Fractal Geometry of Nature. New York: Freeman.

Melcher, J.R., J.J. Guinan, Jr., I.M. Knudson, and N.Y.S. Kiang (1996) Generators of the brainstem auditory evoked potential in cat. II. Correlating lesion sites with waveform changes. Hear. Res. *93:*28–51.

Molnar, C.E., and R.R. Pfeiffer (1968) Interpretation of spontaneous spike discharge patterns of neurons in the cochlear nucleus. Proceed. IEEE *56:*993–1004.

Moore, D.R. (1990) Auditory brainstem of the ferret: Early cessation of developmental sensitivity of neurons in the cochlear nucleus to removal of the cochlea. J. Comp. Neurol. *302:*810–823.

Moore, D.R., and N.E. Kowalchuk (1988) Auditory brainstem of the ferret: Effects of unilateral cochlear lesions on cochlear nucleus volume and projections to the inferior colliculus. J. Comp. Neurol. *272:*503–515.

Moore, J.K., J.K. Niparko, M. Miller, and F. Linthicum (1994) Effect of profound deafness on a central auditory nucleus. Am. J. Otol. *15:*588–595.

Nordeen, K.W., H.P. Killackey, and L.M. Kitzes (1983) Ascending projections to the inferior colliculus following unilateral cochlear ablation in the neonatal gerbil, *Meriones uniguiculatus*. J. Comp. Neurol. *214:*144–153.

Nusser, Z., E. Mulvihill, P. Streit, and P. Somogyi (1994) Subsynaptic segregation of metabotropic and ionotropic glutamate receptors as revealed by immunogold localization. Neuroscience *61:*421–427.

Palay, S.L., and V. Chan-Palay (1974) Cerebellar Cortex, Cytology and Organization. New York: Springer-Verlag.

Panico, J., and P. Sterling (1995) Retinal neurons and vessels are not fractal but space-filling. J. Comp. Neurol. *361:*479–490.

Parks, T.N. (1979) Afferent influences on the development of the brain stem auditory nuclei of the chicken: Otocyst ablation. J. Comp. Neurol. *183:*665–677.

Parks, T.N., D.A. Taylor, and H. Jackson (1990) Adaptations of synaptic form in an aberrant projection to the avian cochlear nucleus. J. Neurosci. *10:*975–984.

Pasic, T.R., D.R. Moore, and E.W. Rubel (1994) Effect of altered neuronal activity on cell size in the medial nucleus of the trapezoid body and ventral cochlear nucleus of the gerbil. J. Comp. Neurol. *348:*111–120.

Pfeiffer, R.R. (1966) Anteroventral cochlear nucleus: Wave forms of extracellularly recorded spike potentials. Science *154:*667–668.

Porter, R., S. Ghosh, G.D. Lange, and T.G. Smith, Jr. (1991) A fractal analysis of pyramidal neurons in mammalian motor cortex. Neurosci. Lett. *130:*112–116.

Powell, T.P.S., and S.D. Erulkar (1962) Transneuronal cell degeneration in the auditory relay nuclei of the cat. J. Anat. *96:*219–268.

Pujol, R., M. Rebillard, and G. Rebillard (1977) Primary neural disorders in the deaf white cat cochlea. Acta Otolaryngol. *83:*59–64.

Ramón y Cajal, R. (1909) Histologie du Système Nerveux de l'Homme et des Vertébrés. Paris: A. Maloine.

Rawitz, B. (1896) Gehörorgan und gehirn eines weissen hundes mit blauen augen. Morphol. Arbeit. *6:*545–554.

Rebillard, M., G. Rebillard, and R. Pujol (1981) Variability of the hereditary deafness in the white cat. I. Physiology. Hear. Res. *5:*179–181.

Recanzone, G.H., C.E. Schreiner, and M.M. Merzenich (1993) Plasticity in the frequency representation of primary auditory cortex following discrimination training in adult owl monkeys. J. Neurosci. *13:*87–103.

Rees, S., F.H. Guldner, and L. Atikin (1985) Activity dependent plasticity of postsynaptic density structure in the ventral cochlear nucleus of the rat. Brain Res. *325:*370–374.

Robertson, D., and D.R. Irvine (1989) Plasticity of frequency organization in auditory cortex of guinea pigs with partial unilateral deafness. J. Comp. Neurol. *282:*456–471.

Rubel, E.W., and T.N. Parks (1988) Organization and development of the avian brain-stem auditory system. In G.M. Edelman, W.E. Gall, and W.M. Cowan (eds): Auditory Function—Neurobiological Bases of Hearing. New York: John Wiley & Sons, pp. 3–92.

Ryugo, D.K. (1992) The auditory nerve: Peripheral innervation, cell body morphology, and central projections. In D.B. Webster, A.N. Popper, and R.R. Fay (eds): Mammalian Auditory Pathway: Neuroanatomy. New York: Springer-Verlag, pp. 23–65.

Ryugo, D.K., and D.M. Fekete (1982) Morphology of primary axosomatic endings in the anteroventral cochlear nucleus of the cat: A study of the endbulbs of Held. J. Comp. Neurol. *210:*239–257.

Ryugo, D.K., and S. Sento (1991) Synaptic connections of the auditory nerve in cats: Relationship between endbulbs of Held and spherical bushy cells. J. Comp. Neurol. *305:*35–48.

Ryugo, D.K., M.M. Wu, and T. Pongstaporn (1996) Activity related features of synapse morphology: A study of the endbulbs of Held. J. Comp. Neurol. *365:*141–158.

Saada, A.A., P.J. Kim, D.R. Vause, J.K. Niparko, and D.K. Ryugo (1995) Auditory nerve activity and structural integrity of cochlear neural elements in the deaf white cat. Assn. Res. Otolaryngol. Abstr. *18:*176.

Saada, A.A., J.K. Niparko, and D.K. Ryugo (1996) Morphological changes in the cochlear nucleus of congenitally deaf white cats. Brain Res. *736:*315–328.

Scheibe, A. (1892) A case of deaf-mutism, with auditory atrophy and anomalies of development in the membranous labyrinth of both ears. Arch. Otolaryngol. *21:*12–22.

Schwartz, I.R., and J.F. Higa (1982) Correlated studies of the ear and brainstem in the deaf white cat: Changes in the spiral ganglion and the medial superior olivary nucleus. Acta Otolaryngol. *93:*9–18.

Seitanidou, T., A. Triller, and H. Korn (1988) Distribution of glycine receptors on the membrane of a central neuron: an immunoelectron microscopy study. J. Neurosci. *8:*4319–4333.

Seldon, H.L., and G.M. Clark (1991) Human cochlear nucleus: Comparison of Nissl-stained neurons from deaf and hearing patients. Brain Res. *551:*185–194.

Sento, S., and D.K. Ryugo (1989) Endbulbs of Held and spherical bushy cells in cats: Morphological correlates with physiological properties. J. Comp. Neurol. *280:*553–562.

Sie, K.C., and E.W. Rubel (1992) Rapid changes in protein synthesis and cell size in the cochlear nucleus following eighth nerve activity blockade or cochlea ablation. J. Comp. Neurol. *320:*501–508.

Smith, T.G., Jr., W.B. Marks, G.D. Lange, W.H. Sheriff, Jr., and E.A. Neale (1989) A fractal analysis of cell images. J. Neurosci. Methods *27:*173–180.

Suga, F., and K.W. Hattler (1970) Physiological and histopathological correlates of hereditary deafness in animals. Laryngoscope *80:*81–104.

Sullivan, W.E., and M. Konishi (1984) Segregation of stimulus phase and intensity coding in the cochlear nucleus of the barn owl. J. Neurosci. *4:*1787–1799.

Treeck, H.H., and W. Pirsig (1979) Differentiation of nerve endings in the cochlear nucleus on morphological and experimental basis. Acta Otolaryngol. *87:*47–60.

Trune, D.R. (1982) Influence of neonatal cochlear removal on the development of mouse cochlear nucleus. I. Number, size, and density of its neurons. J. Comp. Neurol. *209:*409–424.

Waltzman, S.B., N.L. Cohen, and W.H. Shapiro (1992) Use of a multichannel cochlear implant in the congenitally and prelingually deaf population. Laryngoscope *102:*395–399.

Waltzman, S., S. Fisher, J.K. Niparko, and N. Cohen (1994) Predictors of postoperative performance with cochlear implants. Ann. Otol. Rhinol. Laryngol. *165:*15–18.

West, C.D., and J. Harrison (1973) Transneuronal cell atrophy in the deaf white cat. J. Comp. Neurol. *151:*377–398.

Wiesel, T.N., and D.H. Hubel (1963) Effects of visual deprivation on morphology and physiology of cells in the cat's lateral geniculate body. J. Neurophysiol. *26:*973–993.

Wolff, D. (1942) Three generations of deaf white cats. J. Hered. *33:*39–43.